Proceedings of the 11th World Congress on Mechanical, Chemical, and Material Engineering (MCM'25)

Barcelona, Spain -Paris, France - August, 2025

Paper No. HTFF 246 DOI: 10.11159/htff25.246

# Graphite-Enhanced Paraffin and Beeswax Composites: Numerical and Experimental Investigations of Thermal Properties

Mohamed Moussa EL IDI<sup>1,\*</sup>, Atilla ATLI<sup>2</sup>, Ahmad HAJJAR<sup>3</sup>, Manel KRAIEM<sup>4</sup>, Mustapha KARKRI<sup>4</sup>

<sup>1</sup>IMT Nord Europe, Institut Mines Télécom, Center for Energy and Environment, Univ. Lille, 59000, Lille, France <sup>2</sup>ECAM LaSalle, 40 montée Saint-Barthélemy 69321 LYON cedex 05

<sup>2</sup>Center for Environmental Intelligence and College of Engineering and Computer Science, VinUniversity, Ha Noi, Viet

<sup>2</sup>Université Paris- Est, CERTES, 61 Av. du Général de Gaulle, 94010 Créteil Cedex, France Corresponding author: moussa.elidi@gmail.com

**Abstract** - Thermal management is a key factor in ensuring the performance and durability of electronic components as well as electrochemical converters, such as batteries and fuel cells. Phase change materials (PCMs), which undergo phase transitions at a constant temperature or within a narrow temperature range, enable precise and homogeneous thermal control, even in harsh environments, in a passive manner. Environmentally friendly materials are among the most promising candidates for the development of sustainable PCMs. In this context, the present work aims to develop PCM composites based on natural beeswax, characterize their thermophysical properties, and model their thermal behavior. Characterization tests revealed promising results in terms of latent heat and phase change temperature. However, the material's low thermal conductivity limits the phase change kinetics. To address this limitation, graphite microparticles were incorporated. The results show that the addition of 10 wt% graphite (approximately 4.5 vol%) increases thermal conductivity by about 50%. Numerical models were developed and validated through comparison with experimental data.

**Keywords:** Thermal management, PCM, Beeswax, Paraffin

#### 1. Introduction

Due to their high energy densities and high latent heat, phase-change materials (PCMs) have great potential for heat storage [1–3]. However, their low thermal conductivity impacts phase change kinetics, resulting in slow thermal storage and removal [4–7]. This challenge is a significant obstacle to using PCMs in solar and geothermal energy storage. In addition, their low thermal conductivity limits their effectiveness in thermal management applications, such as the thermal management of Li-ion batteries [8,9], PEMFC [10,11] and electronic components [12]. To address these challenges, research, and technological development are being carried out to improve the thermal conductivity of PCMs, making them more efficient thermally.

An effective solution for improving the thermal conductivity of PCMs is to increase their thermal conductivity without significantly reducing their energy densities. One of the most widely studied solutions is to add fins [13,14], metallic foams [15,16] or micro and nanoparticles [17–19]. Microparticles can be divided into carbon (e.g., graphite, graphene, carbon nanotubes), metals (e.g., Cu, Ag), and metal oxides (e.g., CuO, TiO<sub>2</sub>, Al<sub>2</sub>O<sub>3</sub>, and Fe<sub>3</sub>O<sub>4</sub>). Among these particles, graphite particles have attracted considerable attention [20]. PCMs improved by the addition of graphite have been used to recover and valorize industrial waste heat [21].

Zheng et al [22], by adding 5% graphite, were able to reduce the melting time by 13.3%. Adding a percentage of graphite to improve the thermal conductivity of a PCM can impact its melting point and latent heat. Zeng et al. [23] have developed composites of eutectic PCM and expanded graphite. The PCM in question was a mixture of erythritol and mannitol. The results showed that adding 3% graphite reduced the melting temperature by around 2°C, while the latent heat of fusion remained virtually unchanged. K. Khan and Khan [24] studied the impact of micro and nanoparticle materials. The authors conducted experimental and numerical studies on the thermal performance of a storage unit. The PCM used is a paraffin enhanced using different particles, microparticles, and nanoparticles (Al<sub>2</sub>O<sub>3</sub> and Graphite microparticles). All these microparticles were found to improve the phase change kinetics (charge/discharge). Furthermore, particle fractions impact on thermal performance was found to be non-linear. Indeed, increasing the fraction of Al<sub>2</sub>O<sub>3</sub> from 1%vol to 3%vol

significantly improved the system's thermal performance. However, the improvement was slight from 3%vol to 5%vol. Other studies showed that adding micro and nanoparticles is a solution that increases the thermal conductivity of PCM while maintaining a high energy density [3].

The majority of commonly used organic phase change materials (PCMs) are paraffins derived from the oil industry, which have a significant environmental impact. Bio-sourced PCMs offer an eco-friendly alternative. Among them, beeswax stands out due to its wide availability and low cost compared to other bio-based options. Several studies have shown that beeswax exhibits good energy storage capacity, with a latent heat value comparable to that of paraffins.

Based on the studies reviewed above, the aim of this work is to study the thermal performance of a composite combining a Beeswax and graphite microparticles and comparing this composite to a paraffin graphite microparticles composite. For the paraffin, we have selected paraffin RT55, a wax of petroleum origin with a good chemical and thermal stability, as well as a wide phase-change temperature range. Paraffin are not pure substances, which means that they do not change phase at a constant temperature, but rather within a relatively small temperature range [25]. The study is divided into two main parts: the first is experimental, where we have formulated two PCM composites: a paraffin RT55 composite enriched with 10% by mass of graphite microparticles and beeswax composite with the same graphite microparticles fraction, and carried out its experimental thermal conductivity characterization using the Hot-Disk method; the second is numerical, where we have developed a numerical model to predict the thermal conductivity of the PCM/microparticle composite, solved using the finite element method with Ansys software, and carried out parametric studies to assess the influence of graphite thermal conductivity and geometric shape on the effective conductivity of the composite. The results will be presented and discussed.

# 2. Experimental preparation and characterization of PCM-Graphite composites

# 2.1. Elaboration protocol for PCM/graphite microparticles

After a purification step of the beeswax, both the paraffin RT55-graphite and beeswax-graphite composites were prepared using the same protocol. A consistent mass fraction of 10 wt.% graphite microparticles was used in both cases. The preparation procedure involves four main steps:

- **Melting of the pure PCM:** The pure PCM (paraffin RT55 or beeswax) is heated above its melting point until it is fully liquefied.
- Addition of graphite microparticles: 10 wt.% graphite microparticles are then added and thoroughly mixed with the molten PCM (paraffin RT55 or beeswax).

Fig. 1. resume the main steps of the preparation protocol.

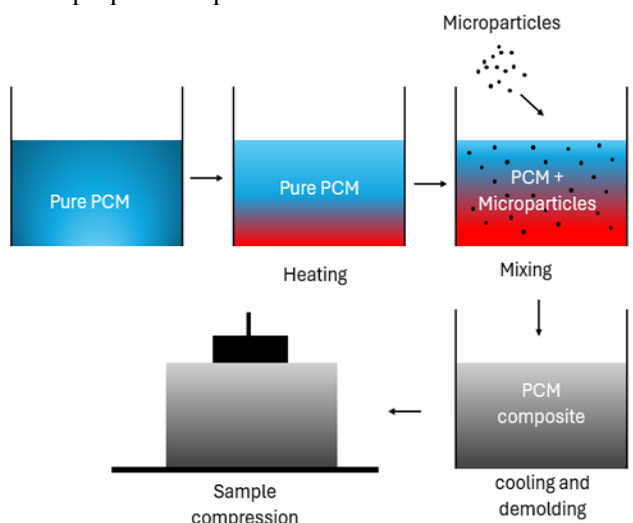


Fig. 1: Experimental elaboration protocol for PCM/graphite microparticles.

Figure 2 presents pure paraffin RT55 and its composite with graphite microparticles, while Figure 3 shows pure beeswax and its corresponding composite with graphite microparticles.



Fig. 2. samples, (a) pure paraffin RT55, (b) paraffin 10 w% graphite composite



Fig. 3. samples, (a) pure beeswax (b) beeswax 10 w% graphite composite

## 2.2. Characterization techniques of the prepared composite-PCM

The Hot-Disk method was used to determine the thermal conductivity of the samples. Specifically, a probe is sandwiched between two samples of the same composition and size. For our study, we used the Hot-Disk TPS 2500. Since the Hot Disk method requires placing the sensor between two identical samples for accurate measurements, the samples were cut accordingly using the experimental setup shown in Fig. 4. The resulting samples are presented in Fig. 5.



Fig. 4. Experimental setup for sample cutting



Fig. 5. Cut samples

## 2.3. Experimental characterization of thermal conductivities using Hot Disk

In order to experimentally evaluate the impact of adding 10% by weight graphite microparticles on the thermal conductivity of beeswax and paraffin RT55, the Hot disk measurements were carried out at the CERTES laboratory using two identical samples. Fig. 6 shows a PT7577 sensor used to characterize the beeswax composite, placed in a sandwich configuration between two identical samples. Fig 7 presents the complete experimental setup.

To ensure repeatability, measurements were repeated 10 times. Table 1 summarizes the results obtained by the Hot Disk. The results show that the thermal conductivity of pure paraffin RT55 is 0.278 W/(m.K), while that of the RT55 paraffin/graphite microparticle composite is 0.345 W/(m.K). This represents a 24% increase in the thermal conductivity of pure paraffin RT55. For pure beeswax, the thermal conductivity is 0.307 W/m·K, and after adding 10% graphite microparticles, it increases to 0.4488 W/m·K, representing a 49% enhancement — approximately twice the improvement observed for RT55 paraffin. These properties were measured in the solid state at 19.5 °C. A complementary characterization in the liquid state will be conducted.



Fig. 6. PT7577 sensor used to characterize the beeswax composite, placed in a sandwich configuration.

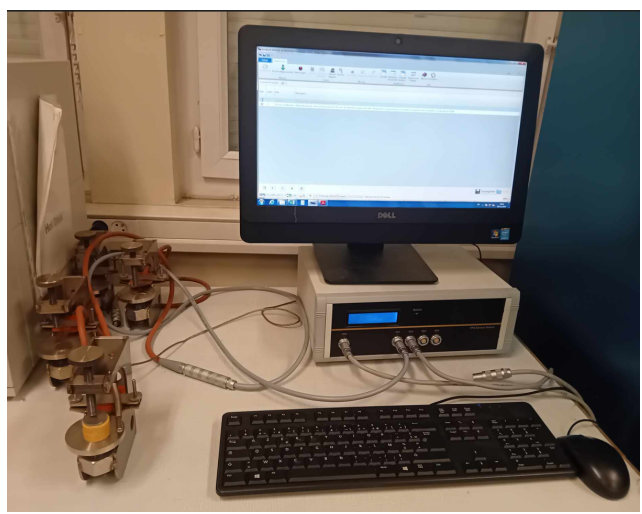


Fig. 7. Experimental protocol.

Table 1: Hot-Disk experimental results

	Pure RT55	RT55 composite	Pure beeswax	Beeswax composite
Thermal	0.278	0.345	0.307	0.4488
conductivity				
$(W.m^{-1}.K^{-1})$				

# 3. Physical model and simulation procedure

# 3.1. Objectives of the simulations

The objective in this section is to determine the composite thermal conductivity through numerical simulations and compare the result to the one obtained experimentally. In addition, the simulations are useful to analyze the heat flow and temperature distribution at the graphite particle scale inside the paraffin.

The thermal conductivities of pure PCMs is determined used experimental devices. Regarding the graphite microparticles, there is no given information about the thermal conductivity of the particles. The thermal conductivity of

synthetic graphite varies in the range  $25-470 \ W/(m.K)$  [26]. In the simulations, the impact of particle thermal conductivity will be evaluated, as well as the particle shape and size.

#### 3.2. Theoretical limits

Before proceeding with the simulations, it is useful to check the theoretical range in which the thermal conductivity of the composite should fall. For that, the two extreme cases are considered: Two PCM-graphite layers in series or in parallel, as shown in Fig. 8.

The thermal resistance of each layer is  $R = L / k_A$ , where L is the layer length, A is the cross-section and k is the thermal conductivity.

Layers in series:

$$A = A_g = A_p \tag{1}$$

$$L = L_{\rho} = L_{\rho} \tag{2}$$

with  $L_g = 0.0416L$  and  $L_p = 0.9584L$ 

$$R_{eq} = R_g + R_p \rightarrow \frac{L}{k_{eq}A} = \frac{L_g}{k_{gAg}} + \frac{L_p}{k_{pAp}} \rightarrow k_{eq} = 3.44 + \frac{0.0416}{k_g}$$
(3)

For any value of  $k_g$  in the range [20 W.m<sup>-1</sup>.K<sup>-1</sup>], 470 W.m<sup>-1</sup>.K<sup>-1</sup>], 0.0416/kg  $\rightarrow$ 0 and  $k_{eq} \approx k_p = 0.278$  W/ (m.K).

Layers in parallel:

$$A = A_{\mathcal{G}} + A_{\mathcal{D}} L = L_{\mathcal{G}} = L_{\mathcal{D}} \tag{5}$$

With  $A_g = 0.0416A$  and  $A_p = 0.9584A$ 

$$\frac{1}{R_{eq}} = \frac{1}{R_g} + \frac{1}{R_p} \xrightarrow{k_{eq}A} \frac{k_{eq}A}{L_g} + \frac{k_{pAP}}{L_p} \rightarrow k_{eq} = 0.2664 + 0.0416 * k_g$$
For  $k_g = 20$  W/ (m.K),  $k_{eq} = 1.09$  W/ (m.K), while for  $k_g = 470$  W/ (m.K),  $k_{eq} = 19.81$  W/ (m.K).

So overall, the lower limit of the composite thermal conductivity is 0.278 W/ (m.K), while its upper limit can reach up to 19.8 W/ (m.K) based on the value of the graphite thermal conductivity.

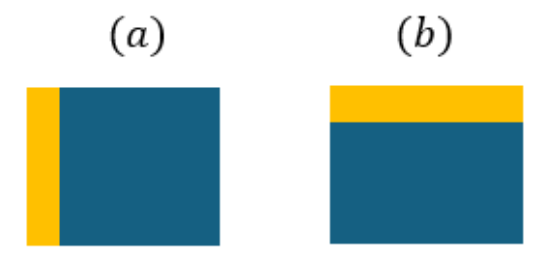


Fig. 8. Two PCM and graphite layers in series (a) or in parallel (b)

## 3.4. Geometrical model and mesh

The numerical simulations are performed using the commercial finite-element software Ansys [27], based on a Representative Volume Element (RVE) approach. First, the geometry is defined: a cube representing the PCM matrix is built, and particles are dispersed inside (Fig. 9). The volume concentration of the particles and their size are set. As a first and simple approach, the particles are considered spherical. The contact between the particles and the PCM matrix is considered bonded and without interphase. In addition, periodic mesh and boundary conditions are applied.

As the particle weight concentration  $\phi_W$  is 10%, their volumetric fraction  $\phi_V$  can be calculated as:

$$\phi_V = \frac{\rho_{pcm} \cdot \phi_W}{\rho_{pcm} \cdot \phi_W + \rho_{graphite} (1 - \phi_W)} = 0.0416 \tag{7}$$

This value is used in the simulations. Once the geometry is set, it is discretized into small elements and the thermal conductivity of the composite  $k_{eq}$  is calculated as the average of the thermal conductivity determined in the three principal directions

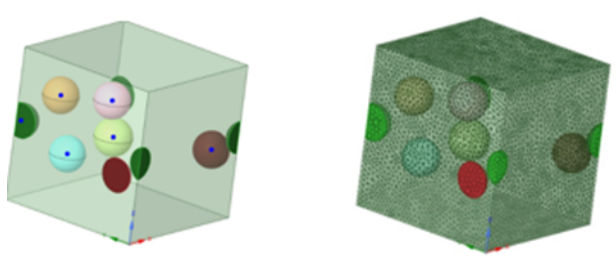


Fig. 9. Representative Volume Element (REV) of the microcomposite with spherical particles

### 4. Results and discussion

In this section, the experimental results of paraffin RT55- graphite microparticles are used to build the model, then the experimental results are compared to numerical ones to validate the model.

#### 4.1. Initial numerical results

A first simulation is performed with some predefined parameters like the particle shape, diameter, and thermal conductivity. This provides a first estimate about the general features of the composite behavior. Subsequently, these parameters can be changed to assess their impacts on the results.

As a first test, a normal distribution is set for the diameter of the particles. The average value is taken as 50  $\mu$ m and the standard deviation is 10  $\mu$ m. The thermal conductivity of the graphite is selected as  $k_{graphite} = 100 \ W/\ (m.K)$ . For these values, the thermal conductivity of the composite was found equal to  $k_{num} = 0.316 \ W/\ (m.K)$ . This value falls well in the theoretical range found in section 1.b. In addition, the value found experimentally  $k_{exp}$  is 9.1% higher that the one obtained in the numerical simulation.

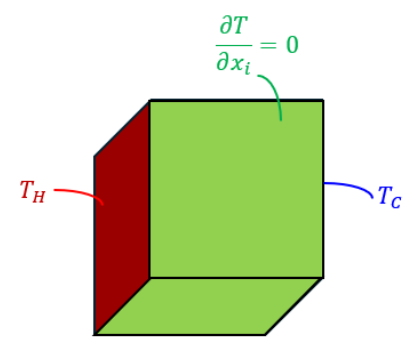


Fig. 10. Boundary conditions of the temperature distribution simulation

#### 4.2. Effect of graphite thermal conductivity

In the first simulation, the thermal conductivity of the graphite was fixed at  $k_g = 100 \ W/$  (m.K). Nonetheless, changing this value can still affect this thermal conductivity, as shown theoretically.

To assess the impact of  $k_g$  on  $k_{num}$ , a set of simulations is performed by keeping the particle shape and size as in section 3.1, but varying the value of  $k_g$  in the range [2-470]W/(m.K). The variation of on  $k_{num}$  as a function of  $k_g$  is illustrated in Fig 11.

# Thermal conductivity of the composite

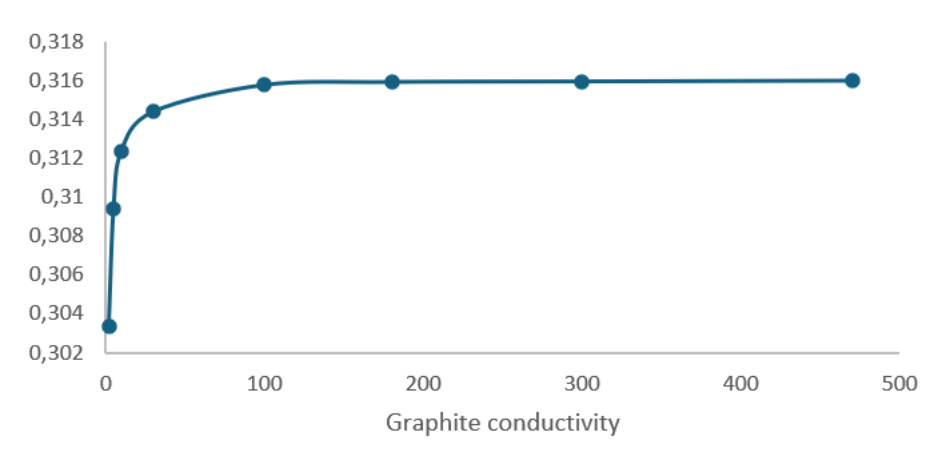


Fig. 11. Variation of the thermal conductivity of the composite as a function of that of the graphite

It is seen that raising  $k_g$  leads to an increase in  $k_{num}$ . However, starting from  $k_g \approx 100$  W/ (m.K), further changes in  $k_g$  do not affect the value of  $k_{eq}$ . This indicates that  $k_g$  is very high compared to  $k_{num}$  such that at some point, the presence of graphite offers no thermal resistance at all and the behavior of the composite becomes independent of the graphite thermal conductivity. In addition,  $k_{num}$  only increases by 4.6% when  $k_g$  is raised from 2 to 100, indicating that even when graphite with low  $k_g$  is used, it still has similar impact as highly conductive graphite.

### 4.3. Analysis of local temperature distribution

In order to analyse the impact of the particles on the heat flux and temperature distribution, the isothermal contours are plotted in the cube, as shown in Figure 12. A high temperature is set at the left wall, while a cold one is on the right wall. The remaining walls are adiabatic, as depicted in Figure 12. A section is then applied to cut the cube, and the isothermals are plotted in both the PCM and the particles.

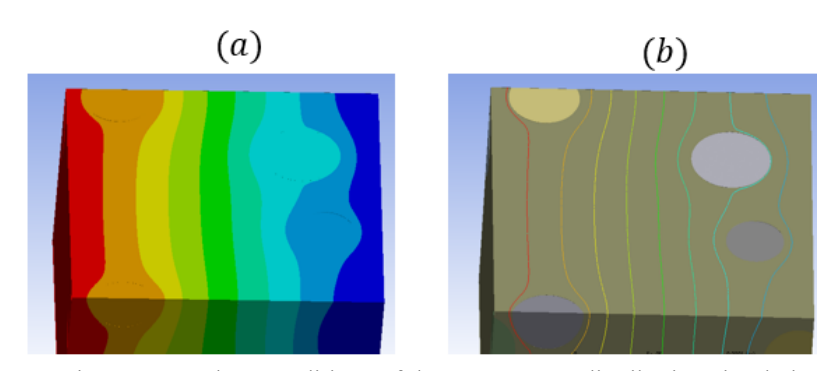


Fig. 12. Boundary conditions of the temperature distribution simulation

It's clear from both the temperature surfaces and contours that the particles affect the temperature patterns. In particular, it is shown that while the temperature is stratified in the PCM zone, it is uniform in every particle. This is due to the high thermal conductivity of the graphite with respect to the paraffin. It is also seen that the sparce distribution of the particles in the cube leads to a localized effect on the temperature contours, such that the overall distribution is not strongly affected. This explains why the change of the thermal conductivity of the composite relative to the composite remains limited.

#### 4.4. Effect of particle diameter and shape

To evaluate the impact of the particle diameter, spherical particles are used but with diameter of 10 microns, with a standard deviation of 5. The corresponding geometry is shown in Figure 13.

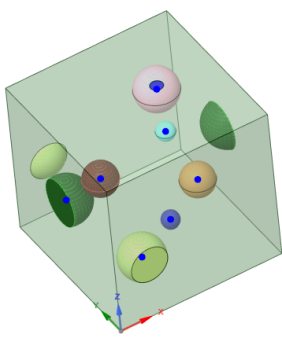


Fig. 13. Geometry used for particle diameter of 5 microns

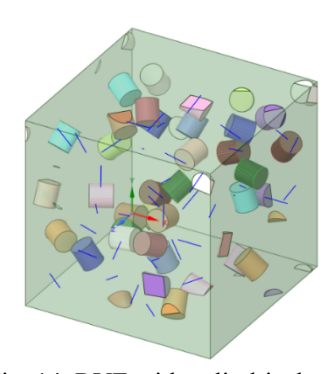


Fig. 14. RVE with cylindrical particles

For this configuration, the thermal conductivity of the composite was found to be  $k_{num} = 0.315 \ W/(m.K)$ , less than 0.3% of what was found with an average particle diameter of 50 microns, which indicates that the particle size has a very small effect on the composite thermal conductivity.

As for particle shape, to address its influence on the composite behaviour, cylindrical shapes are used to replace the spherical ones. Both the diameter and length of each cylinder is set to 10 microns. The corresponding geometry is depicted in Fig 15.

In this case, the composite thermal conductivity was found to be  $0.328 \ W/\ (m.K)$ , which is 3.7% higher than the one found for spherical particles. This slight increase can be attributed to a more uniform distribution of the particles in the PCM matrix. More importantly, this highlights the fact that the particle shape can indeed be one of the reasons of deviation between the numerical and experimental values.

Based on the SEM observations of the graphite microparticles (Fig. 15), it is clear that the particles have in reality a flat geometry, which means that the spherical or cylindrical particle shapes are not fully convenient to represent the particles.

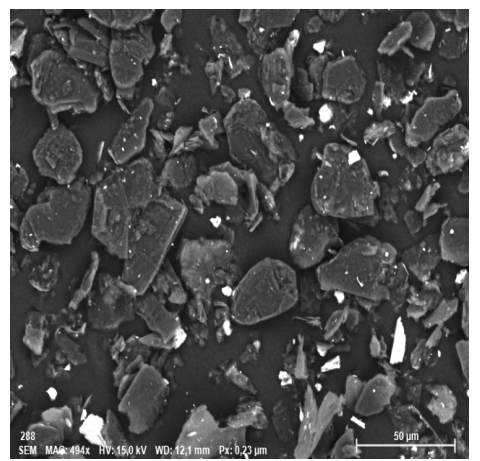


Fig. 15. SEM observation of graphite particles.

For this reason, a model where the particles can be represented by disk-like structures is constructed to better illustrate their flat shape. The model is shown in Fig. 16. The diameter of the disks is set at 50  $\mu$ m, while their thickness is 0.1  $\mu$ m.

For this type of geometry, the equivalent thermal conductivity of the paraffin-based microcomposite is found equal to  $k_{eq} = 0.39 \ W/(m.K)$ , which is 40% higher than the pure PCM, and also 13% higher than the experimental value.





Fig. 16. RVE with disk-like microparticles, at 10% vol concentration

### 4.5. Replacing paraffin by beeswax

The same procedure, presented previously for paraffin PCM, was repeated for Beeswax-graphite composite. In this case, the measured experimental thermal conductivity is  $k_{exp} = 0.44 \ W/(m.K)$ , which is 44% higher than the pure beeswax thermal conductivity  $k_h = 0.307 \ W/(m.K)$ .

The simulations with spherical microparticles, lead to  $k_{eq} = 0.344 \ W/\ (m.K)$ , which is 12% higher than pure beeswax thermal conductivity. It should be noted that the same % increase in thermal conductivity was observed in the case of paraffin with spherical microparticles.

When a model with disk-like particles is used, the obtained equivalent thermal conductivity of the microcomposite becomes  $k_{eq} = 0.43 \ W/\ (m.K)$ , which is 40% higher than the pure PCM and very close to the value obtained experimentally. Table 2 and table 3 summarize the different findings:

Table 2: Summarize experimental and numerical results

<b>D</b> • 4	G ', G' 1, '
Experiment	Composite Simulation
Eaper inient	composite simulation

PCM Material	Pure PCM	Composite	Spherical particles	Disk-like particles
Paraffin	0.278	0.345	0.312	0.39
Beeswax	0.307	0.448	0.344	0.43

Table: 3 Errors

PCM Material	Differe Microocomposite (S PC	, <b>.</b>	Error of the simulation with respect to the experimental result	
TVIALOTIAI	Spherical	Disk	Spherical	Disk
Paraffin	+12%	+40%	-10%	+13%
Beeswax	+12%	+40%	-30%	-2%

# 4.5. Parametric study

In this section, numerical simulations were conducted to investigate the influence of particle geometry on the effective thermal conductivity of paraffin-based micro-PCM composites containing disk-like graphite microparticles.

The mass fraction of graphite was fixed at 10%, and a series of simulations were performed by systematically varying the diameter and thickness of the particles. Three configurations were examined:

- varying particle thickness while keeping diameter constant,
- varying diameter with fixed thickness, and
- varying both diameter and thickness simultaneously while maintaining a constant aspect ratio.

The particles were randomly dispersed within the paraffin matrix.

• Effect of particle thickness for a constant diameter  $d=50 \ \mu m$ : The diameter of the particles was kept constant at 50  $\mu$ m, while the thickness was increased. It is found that the effective thermal conductivity increases with the thickness. This can be due to the fact that a higher particle thickness enhances cross-plane (through-thickness) conduction. Thicker particles provide larger conductive paths in the through-plane direction, improving particle—matrix thermal bridging despite a reduction in total particle number.

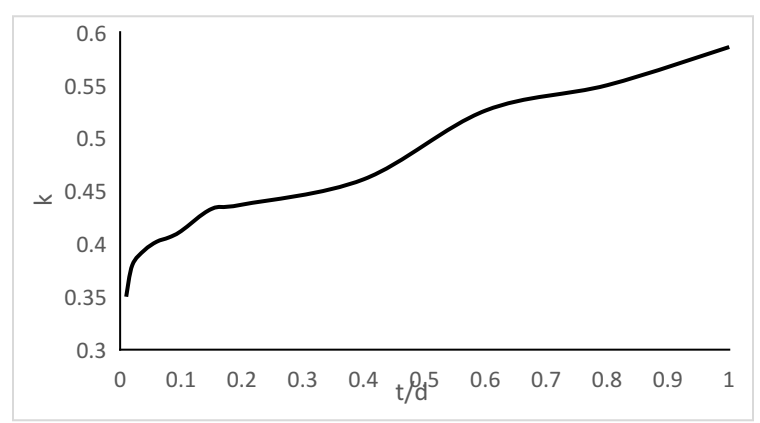


Fig. 17. Variation of the thermal conductivity with the aspect ratio of the disk-like particles

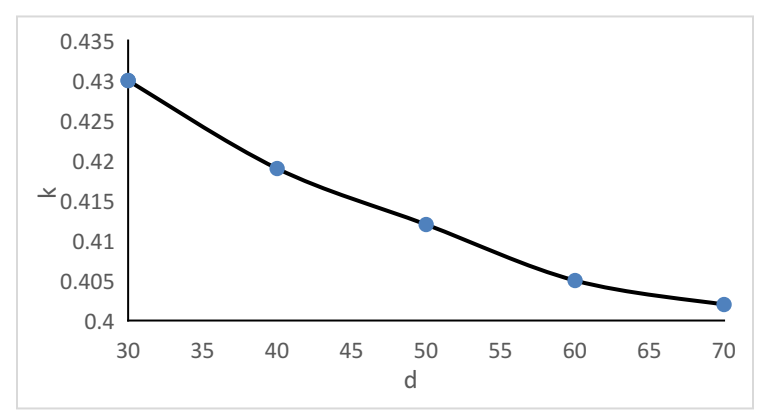


Fig. 18. Variation of the thermal conductivity with the diameter of the disk-like particles with constant thickness

• Effect of particle diameter for a constant thickness  $t=5 \mu m$ : The thickness of the particles was kept constant at 5  $\mu$ m, but the diameter was varied. It is seen that  $k_{eq}$  decreases for higher diameter. In fact, larger diameter particles at constant thickness tend to decrease the number of particles per unit volume for a fixed mass fraction. this reduces the effective surface area for interfacial heat exchange, limiting the formation of conductive networks.

It should be noted that increasing the thickness of the microparticles also reduces the number of particles, but nonetheless enhances  $k_{eq}$ . This improvement is attributed to stronger cross-plane conduction through thicker particles, which more effectively channels heat along the direction of thermal flux. This increase in  $k_{eq}$  is accompanied by a decrease due to lower number of particles, but the net change in  $k_{eq}$  is positive.

• Effect of particle diameter for constant particle volume and aspect ratio t/d = 0.1: Maintaining a constant aspect ratio while increasing both dimensions leads to larger particles overall, which again reduces the particle count and interfacial area density. The reduced density of thermal pathways in the RVE contributes to lower  $k_{eo}$ , despite preserving geometrical proportions.

When both diameter and thickness are increased while maintaining a constant aspect ratio,  $k_{eq}$  decreases. This is due to a significant reduction in particle number and interfacial area, which limits thermal bridging and network formation. These findings suggest that while increased thickness can enhance heat transfer, excessive particle size—regardless of shape—can undermine thermal conductivity by disrupting the thermal percolation network.

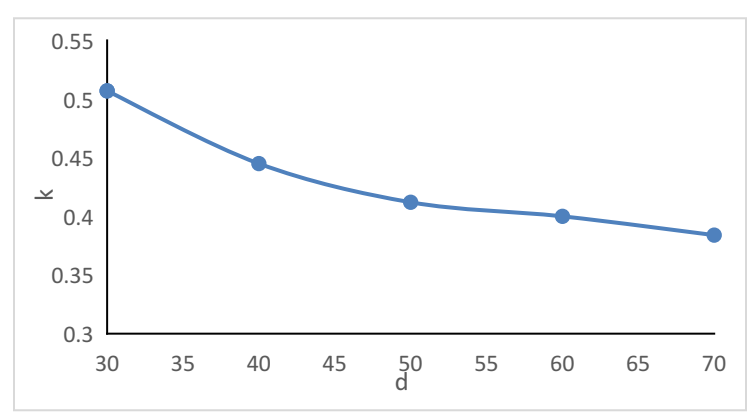


Fig. 18. Variation of the thermal conductivity with the diameter of the disk-like particles with constant aspect ratio

#### 5. Conclusion

In this article, we studied the thermal conductivity of PCM/microparticle composites. This involves adding 10% by mass of graphite to pure paraffin RT55 and beeswax. The Hot-Disk was used to experimentally characterize the thermophysical properties of the PCM composite studied. The results showed an improvement in thermal conductivity of around 24% in the case of paraffin RT55 and 49% in the case of beeswax. A numerical simulation was performed to evaluate the thermal conductivity of the PCM-graphite composite and compare it to the one found experimentally. A RVE was built and the thermal conductivity was determined using finite element simulations in ANSYS. It was found that changing the graphite thermal conductivity beyond a certain limit does not produce any additional effect on the composite thermal conductivity. The numerical result is lower than the experimental one. Depending on the particle shape, the numerical thermal conductivity is between and 9.1% lower than the experimental. It was also obtained that, when the particles are considered spherical, the particle diameter has a negligible impact on the results. Moreover, using cylindrical particles instead of spherical ones increased the thermal conductivity of the composite by 3.7%, which emphasizes the impact of the particle shape on the composite thermal behaviour. Using disk shape to represent the particles led to the best accuracy in comparison to the experimental findings. In fact, the error of numerical results with respect to the experimental results is different based on both the shape of the particles and the PCM. For spherical particles, it's 10% less in paraffin composite simulation compared to experiment, but 30% less for beeswax. But for disk-like particles, it's 13% higher in the paraffin composite, while very good agreement between numerical and experimental results is obtained for the beeswax composite (2%).

Overall, these results show that numerical modeling has the potential to improve and accelerate the predictions of the thermal properties of PCM composites. Further in-depth studies are nonetheless necessary to optimize the simulation models and to provide more comprehensive assessment of the various parameters involved.

The numerical results the importance of both particle geometry and distribution density in optimizing thermal conductivity in micro-enhanced PCMs. While increasing thickness benefits thermal transport via enhanced through-plane conduction, increasing diameter (even proportionally) has a detrimental effect due to decreased particle density and interfacial area. These findings are important for guiding the design of thermally enhanced PCMs using fillers like graphite

### References

- [1] H. Akeiber, P. Nejat, M.Z.Abd. Majid, M.A. Wahid, F. Jomehzadeh, I. Zeynali Famileh, J.K. Calautit, B.R. Hughes, S.A. Zaki, A review on phase change material (PCM) for sustainable passive cooling in building envelopes, Renewable and Sustainable Energy Reviews 60 (2016) 1470–1497. https://doi.org/10.1016/j.rser.2016.03.036.
- [2] G. Alva, L. Liu, X. Huang, G. Fang, Thermal energy storage materials and systems for solar energy applications, Renewable and Sustainable Energy Reviews 68 (2017) 693–706. https://doi.org/10.1016/j.rser.2016.10.021.

- [3] M. Kraiem, M. Karkri, M. Fois, P. Sobolciak, Thermophysical Characterization of Paraffins versus Temperature for Thermal Energy Storage, Buildings 13 (2023) 877. https://doi.org/10.3390/buildings13040877.
- [4] M.M. El Idi, M. Karkri, Heating and cooling conditions effects on the kinetic of phase change of PCM embedded in metal foam, Case Studies in Thermal Engineering 21 (2020) 100716. https://doi.org/10.1016/j.csite.2020.100716.
- [5] M.M. El Idi, A. Hajjar, A. Atli, L. Boussaba, M. Kraiem, M. Abdou Tankari, M. Karkri, Chapter Six Metal foambased PCM, in: H. Muhammad Ali (Ed.), Advanced Materials-Based Thermally Enhanced Phase Change Materials, Elsevier, 2024: pp. 131–192. https://doi.org/10.1016/B978-0-443-21574-2.00006-X.
- [6] X. Man, H. Lu, Q. Xu, C. Wang, Z. Ling, Review on the thermal property enhancement of inorganic salt hydrate phase change materials, Journal of Energy Storage 72 (2023) 108699. https://doi.org/10.1016/j.est.2023.108699.
- [7] L. Nguyen, B. Alshuraiaan, A. Hajjar, M. Izadi, M.M. El Idi, Controlling energy loss from roof structures equipped by round-corner double semi-hexagonal ferro- phase change material layer using magnetic field, Journal of Cleaner Production 428 (2023) 139335. https://doi.org/10.1016/j.jclepro.2023.139335.
- [8] M.M. El Idi, M. Karkri, M. Abdou Tankari, A passive thermal management system of Li-ion batteries using PCM composites: Experimental and numerical investigations, International Journal of Heat and Mass Transfer 169 (2021) 120894. https://doi.org/10.1016/j.ijheatmasstransfer.2020.120894.
- [9] M.M. El idi, M. Karkri, M. Abdou tankari, S. Vincent, Hybrid cooling based battery thermal management using composite phase change materials and forced convection, Journal of Energy Storage 41 (2021) 102946. https://doi.org/10.1016/j.est.2021.102946.
- [10] M.M. El Idi, M. Ankouni, R. Ben Haj Slama, P. Affonso Nobrega, A. Hajjar, A. Atli, Critical review of the latest advances in thermal management techniques for PEM fuel cells, Renewable and Sustainable Energy Reviews 226 (2026) 116199. https://doi.org/10.1016/j.rser.2025.116199.
- [11] M.M.E. Idi, PEMFC Passive Thermal Management Systems: A Review, (2023). https://doi.org/10.20944/preprints202306.2169.v1.
- [12] M.M. El Idi, M. Karkri, M. Abdou Tankari, Chapter 14 Passive thermal management systems for e-mobility using PCM composites, in: F. Aloui, E.G. Varuvel, A. Sonthalia (Eds.), Handbook of Thermal Management Systems, Elsevier, 2023: pp. 323–369. https://doi.org/10.1016/B978-0-443-19017-9.00032-5.
- [13] Kh. Hosseinzadeh, M. Alizadeh, M.H. Tavakoli, D.D. Ganji, Investigation of phase change material solidification process in a LHTESS in the presence of fins with variable thickness and hybrid nanoparticles, Applied Thermal Engineering 152 (2019) 706–717. https://doi.org/10.1016/j.applthermaleng.2019.02.111.
- [14] M. Kazemi, M.J. Hosseini, A.A. Ranjbar, R. Bahrampoury, Improvement of longitudinal fins configuration in latent heat storage systems, Renewable Energy 116 (2018) 447–457. https://doi.org/10.1016/j.renene.2017.10.006.
- [15] M.M. El idi, M. Karkri, M. Kraiem, Preparation and effective thermal conductivity of a Paraffin/ Metal Foam composite, Journal of Energy Storage 33 (2021) 102077. https://doi.org/10.1016/j.est.2020.102077.
- [16] M. Caliano, N. Bianco, G. Graditi, L. Mongibello, Analysis of a phase change material-based unit and of an aluminum foam/phase change material composite-based unit for cold thermal energy storage by numerical simulation, Applied Energy 256 (2019) 113921. https://doi.org/10.1016/j.apenergy.2019.113921.
- [17] M.A. Ali, Fayaz, R.F. Viegas, M.B. Shyam Kumar, R.K. Kannapiran, M. Feroskhan, Enhancement of heat transfer in paraffin wax PCM using nano graphene composite for industrial helmets, Journal of Energy Storage 26 (2019) 100982. https://doi.org/10.1016/j.est.2019.100982.
- [18] Y. Xia, W. Cui, H. Zhang, Y. Zou, C. Xiang, H. Chu, S. Qiu, F. Xu, L. Sun, Preparation and thermal performance of n-octadecane/expanded graphite composite phase-change materials for thermal management, J Therm Anal Calorim 131 (2018) 81–88. https://doi.org/10.1007/s10973-017-6556-1.
- [19] M.M. El Idi, M. Karkri, Méthode inverse pour la détermination expérimentale des propriétés thermophysiques des matériaux à changement de phase, in: Congrès Français de Thermique, SFT 2018, PAU, France, 2018. https://hal.science/hal-02402478 (accessed August 23, 2025).

- [20] M. Dhandayuthabani, S. Jegadheeswaran, V. Vijayan, A.G. Antony, Investigation of latent heat storage system using graphite micro-particle enhancement, J Therm Anal Calorim 139 (2020) 2181–2186. https://doi.org/10.1007/s10973-019-08625-7.
- [21] T. Xiong, Y.S. Ok, P.D. Dissanayake, D.C.W. Tsang, S. Kim, H.W. Kua, K.W. Shah, Preparation and thermal conductivity enhancement of a paraffin wax-based composite phase change material doped with garlic stem biochar microparticles, Science of The Total Environment 827 (2022) 154341. https://doi.org/10.1016/j.scitotenv.2022.154341.
- [22] Z.-J. Zheng, M.-J. Li, Y.-L. He, Optimization of porous insert configurations for heat transfer enhancement in tubes based on genetic algorithm and CFD, International Journal of Heat and Mass Transfer 87 (2015) 376–379. https://doi.org/10.1016/j.ijheatmasstransfer.2015.04.016.
- [23] J.L. Zeng, Y.Y. Liu, Z.X. Cao, J. Zhang, Z.H. Zhang, L.X. Sun, F. Xu, Thermal conductivity enhancement of MWNTs on the PANI/tetradecanol form-stable PCM, J Therm Anal Calorim 91 (2008) 443–446. https://doi.org/10.1007/s10973-007-8545-2.
- [24] Z. Khan, Z. Ahmad Khan, Experimental and numerical investigations of nano-additives enhanced paraffin in a shell-and-tube heat exchanger: A comparative study, Applied Thermal Engineering 143 (2018) 777–790. https://doi.org/10.1016/j.applthermaleng.2018.07.141.
- [25] H. Togun, H.S. Sultan, H.I. Mohammed, A.M. Sadeq, N. Biswas, H.A. Hasan, R.Z. Homod, A.H. Abdulkadhim, Z.M. Yaseen, P. Talebizadehsardari, A critical review on phase change materials (PCM) based heat exchanger: Different hybrid techniques for the enhancement, Journal of Energy Storage 79 (2024) 109840. https://doi.org/10.1016/j.est.2023.109840.
- [26] L. Zhao, J. Tang, M. Zhou, K. Shen, A review of the coefficient of thermal expansion and thermal conductivity of graphite, New Carbon Materials 37 (2022) 544–555. https://doi.org/10.1016/S1872-5805(22)60603-6.
- [27] Ansys Logiciel de simulation numérique, (n.d.). https://www.ansys.com/fr-fr (accessed August 23, 2025).